Am J Transl Res 2019;11(4):2403-2412
www.ajtr.org /ISSN:1943-8141/AJTR0093297

Original Article

Decreased levels of superoxide dismutase in inner pillar cells contribute to ribbon synapse impairment in presbycusis

Haolin Wang[1*], Yuhong Qin[1*], Yue Zhang[2], Wanming Cui[1], Yu Lei[1], Xiaorui Ma[3], Yu Cheng[1], Lin Shi[1], Mei Lv[1]

[1]Department of Otolaryngology, The First Affiliated Hospital of Dalian Medical University, Dalian 116013, China; [2]The Institute of Otolaryngology, Chinese PLA General Hospital, Beijing 100853, China; [3]Department of Otolaryngology, Taiyuan Central Hospital of Shanxi Medical University, Taiyuan 030000, China. [*]Equal contributors.

Received March 3, 2019; Accepted March 26, 2019; Epub April 15, 2019; Published April 30, 2019

Abstract: Objective: To determine if decreased Cu/Zn superoxide dismutase (SOD1) levels in inner pillar cells is associated and diminished inner hair cell ribbon synapse plasticity in presbycusis. Methods: We evaluated the auditory brainstem responses (ABRs) of 2-, 5-, 6-, and 7-month-old C57BL/6J mice. ABRs were obtained using clicks and 4-, 12-, and 32-kHz tone bursts. Cochleae were collected immediately after audiometric assessment for Western blot analysis. The inner and outer hair cells and the inner hair cell ribbon synapses were separately counted. Frozen tissue sections were exposed to immunofluorescent staining for examine of SOD1 expression in the cochlea. Results: ABR thresholds were elevated in the 6- and 7-month groups. The maximal elevation was detected at 32 kHz. Distortion product otoacoustic emission amplitudes decreased in the mice at 5 months. SOD1 levels in the cochlea decreased as the mice aged. A reduction of SOD1 in the inner pillar cells was detected. Hair cell counting showed an apparent decrease in OHCs from 6 months onwards. The mean number of ribbon synapses was 17.2 ± 1.4, 17.7 ± 2.74, 12.8 ± 0.95, and 9.7 ± 3.08 in the 2-, 5-, 6-, and 7-month groups, respectively. This number significantly decreased with increasing age ($P < 0.05$). Conclusion: Our study revealed that age-related hearing loss (ARHL) of C57BL/6J mice was caused by multi-site degeneration in the cochlea. Decreased expression of SOD1 in the cochlea is consistent with changes in the hearing threshold. Decreased SOD1 levels in the inner pillar cells may lead to diminished basilar membrane vibration and a reduction in the number of ribbon synapses, which plays an essential role in age-related hearing loss (ARHL).

Keywords: Age-related hearing loss, SOD, hair cell, ribbon synapse, inner pillar cells

Introduction

Presbycusis or age-related hearing loss (ARHL) is the most frequent neurodegenerative disorder and communication deficit in the elderly [1]. ARHL has a multifactorial etiology that includes overexposure to sound, certain drugs, and aggravating factors, such as diabetes and hypertension. While the cumulative damage resulting from long-term exposure to noise or other insults greatly contributes to the development of presbycusis [2], ARHL has been observed even without such exposures, such as animals raised in quiet environments [3]. Reactive oxygen species (ROS) and reactive nitrogen species (RNS) have also been implicated in the age-related decline of auditory function. The free radical theory attributes aging to the cumulative damage caused by ROS [4, 5]. Animal studies have shown that a deficiency of antioxidant enzymes accelerates the aging process. For example, the age-related loss of cochlear hair cells is significantly higher in mice that do not express superoxide dismutase 1 (SOD1) [6], and susceptibility to noise-induced loss of hearing is enhanced in mice that lack glutathione peroxidase 1 (GPX1) and SOD1 [7, 8].

Research on the cochlear pathologies underlying presbycusis has provided insight into the associated molecular pathways and has impli-

cated the inner hair cell (IHC) ribbon synapses as the primary target of these pathways [9]. Inner pillar cell (IPC) microtubules are connected to sensory hair cells by substantial cell junctions at the pillar cell apices, which opens ion channels in the IHCs membrane indirectly. The consequent influx of current through these channels alters the membrane potential, which in turn affects the rate of release of the ribbon synapse from the IHC of a synaptic transmitter [10]. Damage to the IHCs or adjacent areas disrupts neurotransmission at the ribbon synapses, which is essential for hearing. The ribbon synapses have been shown to be the primary pathological target in noise- and gentamicin-induced auditory dysfunction [11-13], and some researchers believe that a change in ribbon synapse plasticity is the first step in the development of presbycusis [14].

However, the relationship between SOD1 deficiency and ribbon synapse loss remains unknown. It is also not definitively known whether the ribbon synapse is the primary target organ in ARHL. Therefore, the aim of this study was to determine the association of SOD1 deficiency with ribbon synapse loss and ARHL in mice. We found that not only metabolic disorders could cause reductions in releasing the ribbon synapse, but also apparent changes in SOD levels in IPCs was detected, which may affect nerve transduction in another manner.

Materials and methods

Experimental animals

C57BL/6J mice aged 2, 5, 6, and 7 months were obtained from the Experimental Animal Center of Dalian Medical University. Twenty mice weighing 20-30 g each with a normal auricular reflex were chosen from each age group, regardless of gender. Mice with middle ear or inner ear diseases were excluded. This study complied with the Guide for the Care and Use of Laboratory Animals of the National Institutes of Health. Ethical approval for the experimental protocol was granted by the ethics committee of Dalian Medical University. All surgeries were performed under anesthesia and all possible efforts were made to minimize the suffering of animals.

Experimental procedure

Mice were sedated with ketamine (100 mg/kg, i.p.) and xylazine (10 mg/kg, i.p.) at a dose of 0.1 mL/kg (Sigma, San Francisco, CA, USA) before the audiometry assessments. We first examined the auditory function of the mice by using click hearing thresholds, tone bursts, and distortion product otoacoustic emissions (DPOAEs). The mice were then decapitated under deep anesthesia. The cochleae were surgically removed. One cochlea of each mouse was made into a surface preparation. Part of the other cochlea was stored at -80°C and subsequently used for Western blot analysis. The remainder of the cochlear tissue was used for frozen section analysis and immunohistochemistry analysis. In this study, 10 cochleae of each group were used for Western blot analysis, and 10 cochleae were used for frozen section analysis. For surface preparations and frozen sections, the round and oval windows of the cochlea were opened and perfused overnight with 4% paraformaldehyde.

Auditory assessments

Auditory brainstem response (ABR) audiometry was performed for both ears (Intelligent Hearing Systems, Miami, FL, USA). The assessors were blinded to the animal groups. We used the Smart-EP software (v2.21, Intelligent Hearing Systems, Miami, FL, USA) to generate specific acoustic stimuli as well as to amplify, measure, and display the evoked brainstem responses. We placed the reference electrode on the vertex, the recording electrode on the mastoid of the ear being tested, and the ground electrode on the contralateral ear (**Figure 1A**). Auditory stimuli consisting of broadband clicks and 4-, 12-, and 32-kHz tone bursts were delivered to the animals via insert earphones (Intelligent Hearing Systems, Miami, FL, USA). Auditory thresholds based on wave III visibility and reproducibility was determined by changing the sound-pressure levels in 5-dB increments and decrements. The auditory threshold was defined as the lowest level that elicited a recognizable ABR (at least two reproducible peaks; **Figure 1B**).

We measured DPOAEs with an ER-10B+ microphone (Etymotic Research, Elk Grove Village, IL, USA) and two EC1 speakers. We used stimuli consisting of the primary tones f1 and f2, such that the ratio of f2 to f1 was 1.2. The intensities of f1 and f2 were 65 dB and 55 dB, respectively. These intensities were increased from 8 kHz to 32 kHz in 1/2-octave increments. The stimuli were digitally generated and attenuated

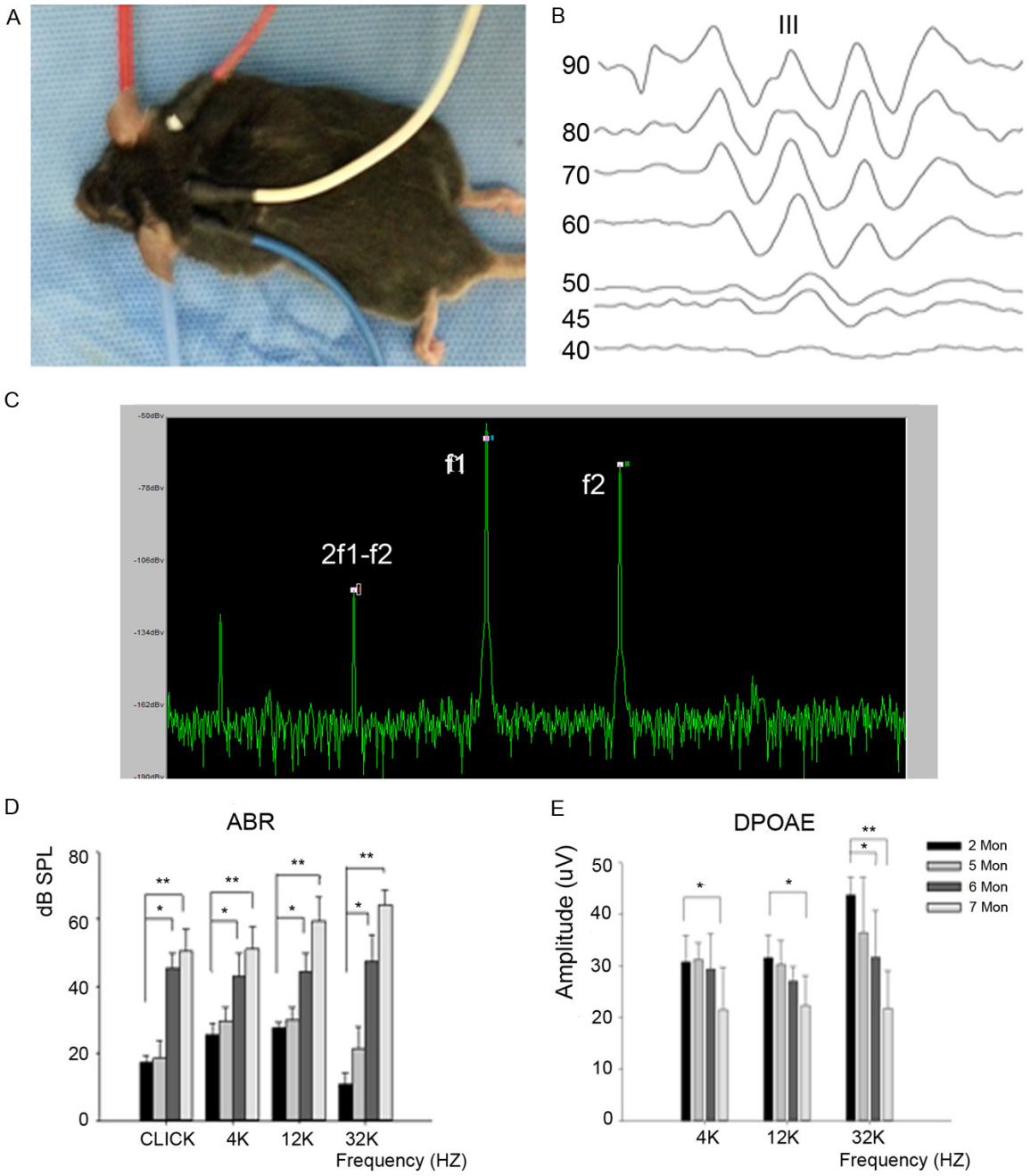

Figure 1. Auditory brainstem response (ABR) and distortion product otoacoustic emission (DPOAE) amplitudes in the four groups. A. Electrode placement. B. ABR waveforms evoked by clicks showing how to determine the hearing threshold with wave III. C. DPOAE assessment, with f1 and f2 connected to the earpiece. The f2 was set at 4, 8, 16, and 32 kHz. The f2/f1 ratio was set at 1.2. The intensity of f2 was 55 dB, and that of f1 was 65 dB. Amplitudes of 2f1-f2 were measured. D. The hearing threshold is elevated in the 6- and 7-month groups, especially at high frequencies (*$P < 0.05$, **$P < 0.01$). E. DPOAE amplitudes are decreased in the 5-month group. The amplitudes for high frequencies decreased first (*$P < 0.05$, **$P < 0.01$).

(200-kHz sampling). The sound pressure in the ear canal was pre-amplified and digitized. We measured amplitudes of 2f1-f2 against the baseline (**Figure 1C**).

Western blot analysis

Western blot analysis was used to determine the SOD1 levels in the cochleae of mice. The

analysis was performed using an automated device (Wes Simple Western Analysis, Protein Simple, San Jose, CA, USA) according to the manufacturer's instructions. We performed initial titrations to optimize the antibody and total protein concentrations for each protein. In brief, the cochlea were washed with saline, frozen in liquid nitrogen, and stored at -80°C until analysis. For this assay, the cochlear tissue samples were pulverized and centrifuged for 10 min at 1,000 *g* and 4°C. The precipitate was quantitatively analyzed using BCA kits (Biyuntian, Shanghai, China) and the Protein Simple Wes System (capillary method). The internal reference was actin (Abcam, Cambridge, UK), and the primary antibody was goat anti-mouse SOD1 polyclonal antibody (Abcam, 1:100, ab6-2800, Cambridge, UK).

Cochlear tissue processing

As stated earlier, one cochlea of each mouse was made into a surface preparation. For this purpose, the cochlear shell was decalcified in 10% ethylenediaminetetraacetic acid (EDTA) for 8 h. Then, the basal turn was separated in 0.01 mmol/L phosphate-buffered saline (PBS) under a dissection microscope. Next, the apical turn was separated, and the vestibular and tectorial membranes were removed.

The other cochlea was decalcified in 10% EDTA for 4 days and subsequently made into a frozen section. After the decalcification, the cochlea was washed in PBS and placed overnight in a 30% saccharose solution under agitation at 4°C for cryoprotection of the tissue. Appropriately oriented frozen specimens of the inner ear were sectioned at 40-μm intervals, mounted on slides, dried, and cover slipped.

Immunohistochemistry and confocal microscopy

The basilar membrane was washed thrice in 0.01 M PBS and pre-incubated in a blocking solution (5% normal donkey serum in 0.01 M PBS) for 30 min at room temperature. After this, the slide was incubated overnight at 4°C with the following primary antibodies: rabbit anti-mouse anti-C terminal-binding protein 2 (CtBP2) antibody (dilution, 1:200; ab128871, Abcam, Cambridge, UK) and goat anti-mouse SOD1 monoclonal antibody (1:200) antibody. The specimens were again washed thrice in 0.01 M PBS and then incubated for 60 min at room temperature with the following fluorescein isothiocyanate-conjugated antibodies: donkey anti-rabbit 488 (dilution, 1:100; ab150073, Abcam, Cambridge, UK) and donkey anti-goat 568 (dilution, 1:100; ab175704, Abcam, Cambridge, UK). Next, the specimens were again washed thrice. The basilar membrane was stained with 4,6-diamidino-2-phenylindole (DAPI; Santa Cruz, San Antonio, TX, USA), cover slipped, and examined under a dissection microscope.

To detect the ribbon synapse, we examined the samples by using fluorescent microscopy. We counted the number of spots that were positive for RIBEYE/CtBP2 by examining the specimens under a laser scanning confocal microscope (Olympus FV1000, Tokyo, Japan) equipped with a 180× oil immersion objective lens. Scanning was performed with excitation wavelengths of 488 nm and 647 nm. As mature IHC ribbon synapses typically measure 150-200 nm, we selected a scanning interval of 0.2 mm to ensure that each synapse was counted.

The frozen sections were stained in the same way as above, with the following antibodies: goat anti-mouse SOD1 polyclonal antibody (dilution, 1:100) and donkey anti-goat 488 (dilution, 1:200). The frozen sections were placed in Vectashield (Vector Laboratories, Burlingame, CA, USA) with DAPI to stain the nuclei, cover slipped, and examined using a fluorescent microscope.

Cochlear ribbon synapse counting

We examined two-dimensional images obtained using serial scanning to identify and count the IHC ribbon synapses. Serial scans from top to bottom were examined using the 3Ds Max software (Olympus, Tokyo, Japan). We magnified the images by using the 'zoomed top view' tool of the software. Green fluorescent spots, which indicated pre-synaptic ribbons, were identified on each image by placing a round marker on the spot. The size of the marker was adjusted to match the area of the spot. Every image served as the reference for the subsequent image, and green fluorescent spots counted in the previous image were skipped in the next image if they were in the same location. Furthermore, only two consecutive images could overlap. After examining all the images, we calculated

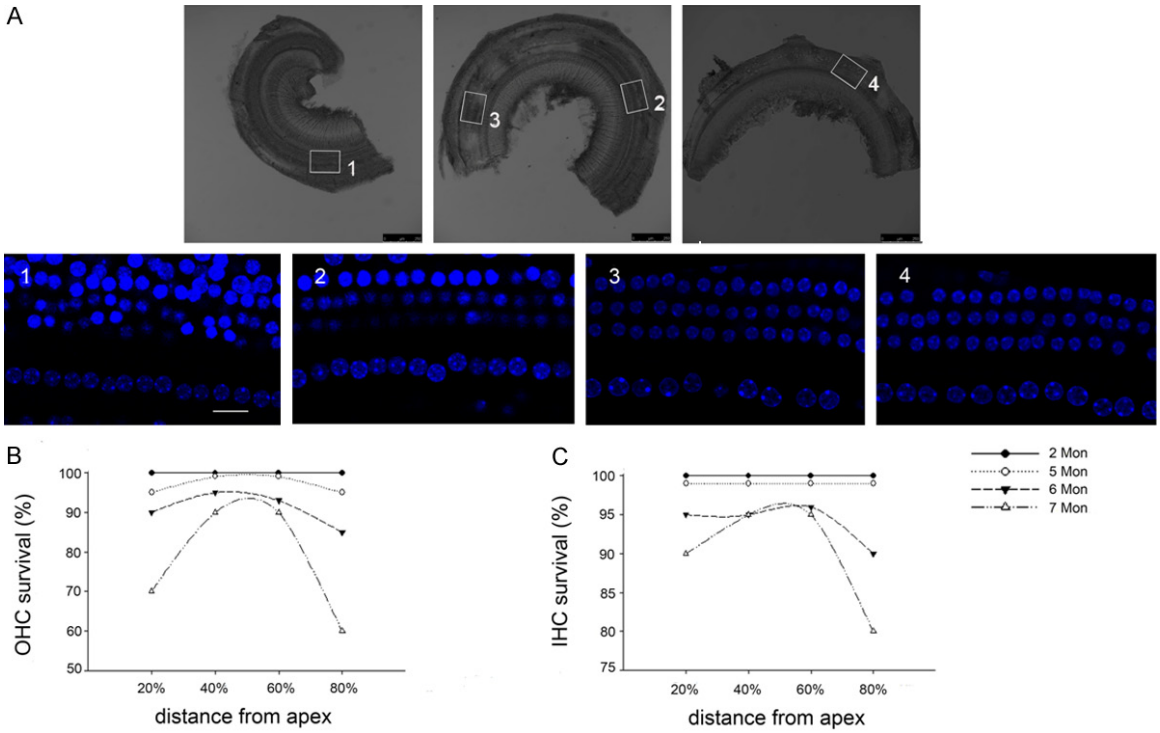

Figure 2. Hair cell counts in different month groups. A. The method and the site in the cochlea to count OHC and IHC. We counted the hair cells within areas situated at 20%, 40%, 60%, and 80% of the distance from the apex of the basilar membrane (bar = 250 μm). B. OHCs in the low- and high-frequency areas (20% and 80% from apex to bottom) on the basilar membrane are slightly decreased in the 6-month group (89.7% and 84.5% cells survival, respectively) and significantly decreased in the 7-month group. The number of OHCs in the middle turn was relatively stable (bar = 25 μm). C. In the 6-month group, high-frequency IHCs lose 21.1%, the decrease in low frequency was not statistically significance (4.6%, $P > 0.05$). Apparent IHC disruption was detected from 7 months onwards and was confined to the high-frequency areas.

the total number of spheres by using the layer manager of the 3Ds Max software [11].

Hair cell counting

The hair cells in the confocal images were counted using the Image J 1.45s software. All the IHCs and outer hair cells (OHCs) in a 160×65 mm area were counted under a 60/1.4 NA objective lens of a confocal microscope. DAPI-labeled cells were identified as hair cells, and IHCs and OHCs were differentiated by their morphological features and their positions relative to supporting cells. We counted the hair cells within areas situated at 20%, 40%, 60%, and 80% of the distance from the apex of the basilar membrane (**Figure 2A**). Five images were examined for each cochlea.

Statistical analysis

All statistical analyses were performed using SPSS (IBM Corporation, Somers, NY, USA). Data were expressed as mean ± SEM. The ABR audiograms (specifically SPL thresholds) of each age group were compared across frequencies and within individual frequencies by using the one-way analysis of variance (ANOVA) and the Tukey post-hoc multiple comparison test. Hair cell counts at different distances in the cochlea were analyzed using two-way ANOVA and the Student *t*-test with the Bonferroni correction. The number of synapses was compared using one-way ANOVA. *P*-values < 0.05 indicated statistical significance. The correlation between the number of synapses and the ABR thresholds was examined using linear regression analysis.

Results

Changes in ABR audiograms

Click-induced ABR thresholds increased with age from 2 to 7 months as follows: 17.25 ±

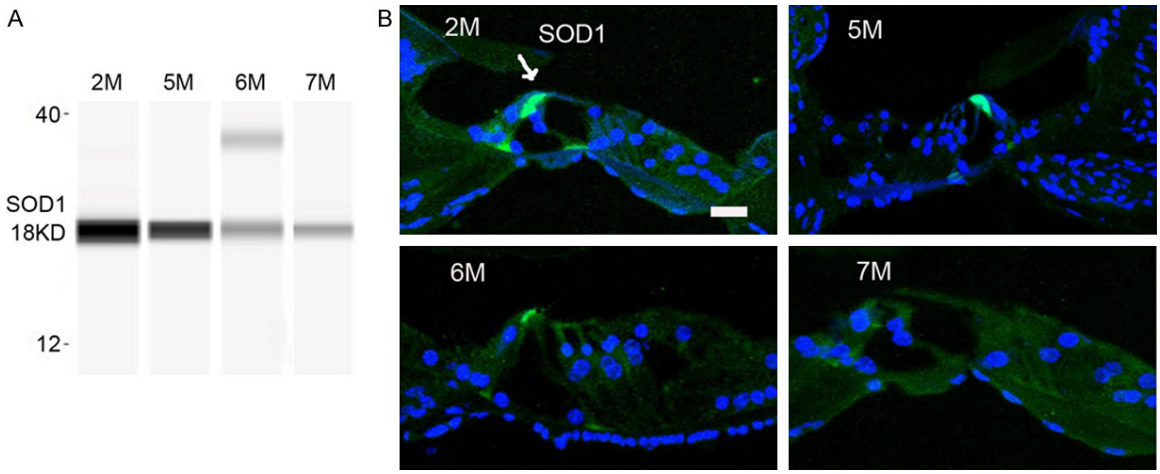

Figure 3. SOD1 content in the cochlea. A. SOD1 content in the cochlea was quantified using Western blot analysis. The amount of SOD1 decreased with age. B. In the organ of Corti, SOD1 was expressed primarily in the inner hair cells and inner pillar cells. SOD1 deficiency was detected in the 6-month and 7-month groups (bar = 25 μm).

2.55, 18.75 ± 4.55, 33.0 ± 4.97, and 47.25 ± 4.13 dB SPL. Significant increases in ABR thresholds were seen from 6 months onward ($P < 0.05$; **Figure 1D**). The maximal threshold elevation was detected at 32 kHz. The ABR thresholds for 32-kHz tone bursts in the four age groups (from 2 to 7 months) were 14 ± 3.08, 23.75 ± 6.46, 40.75 ± 6.74, and 62.75 ± 4.12 dB SPL, respectively ($P < 0.05$; **Figure 1D**).

Unlike the ABR thresholds, DPOAE amplitudes decreased much earlier. The DPOAEs in the 5-month group at 4, 12, and 32 kHz were 31.3 ± 3.2, 30.3 ± 4.6, and 36.5 ± 10.7 μV, respectively. The amplitude of the highest frequency decreased first. The mid- and low-frequency DPOAEs decreased with increasing age ($P < 0.05$; **Figure 1E**).

Changes in SOD1 content in the cochlea and organ of Corti

We examined the SOD1 levels in the cochlea by Western blot analysis. A gradual decrease occurred with increasing age (**Figure 3A**). Frozen sections showed normal morphology of the organ of Corti. SOD1 was broadly expressed in the organ of Corti, but highly accumulated in the hair cells and support cells, especially in the IPC. SOD1 expression in the organ of Corti decreased from 6 months onwards (**Figure 3B**). Although we could not visualize the IPC nucleus due to its deep location (**Figure 4A**), we could detect a consistent age-dependent decrease of SOD1 in the IPCs when observed in the cochlear sections (**Figure 4B**).

Changes in hair cell counts

An analysis of the hair cell counts showed that the number of OHCs in the low- and high-frequency areas (20% and 80% from apex to bottom, respectively, **Figure 2B**) on the basilar membrane had no statistically change until 6 months (in the basal turn, only 84.5% cells survival, $P < 0.05$). The middle-turn OHC counts were relatively stable (**Figure 2B**). Apparent IHC disruption was detected from 7 months, but only the high-frequency area was affected (**Figure 2C**). The rate and extent of IHC reduction were lower than those of OHC reduction.

Changes in ribbon synapses

We identified IHC-spiral ganglion neuron (SGN) synapses with an antibody against RIBEYE/CtBP2, which is a pre-synaptic protein specific to ribbon synapses (**Figure 4B**). We counted 10 IHCs each from the apical, middle, and basal turns (total, 30 IHCs) in each cochlea. The number of synapses did not significantly differ between the different turns ($P > 0.05$). The mean number of ribbon synapses was 17.2 ± 1.4, 17.7 ± 2.74, 12.8 ± 0.95, and 9.7 ± 3.08 per IHC in the 2-, 5-, 6-, and 7-month groups, respectively (**Figure 4B**, **4C**). This number significantly decreased with increasing age ($P < 0.05$).

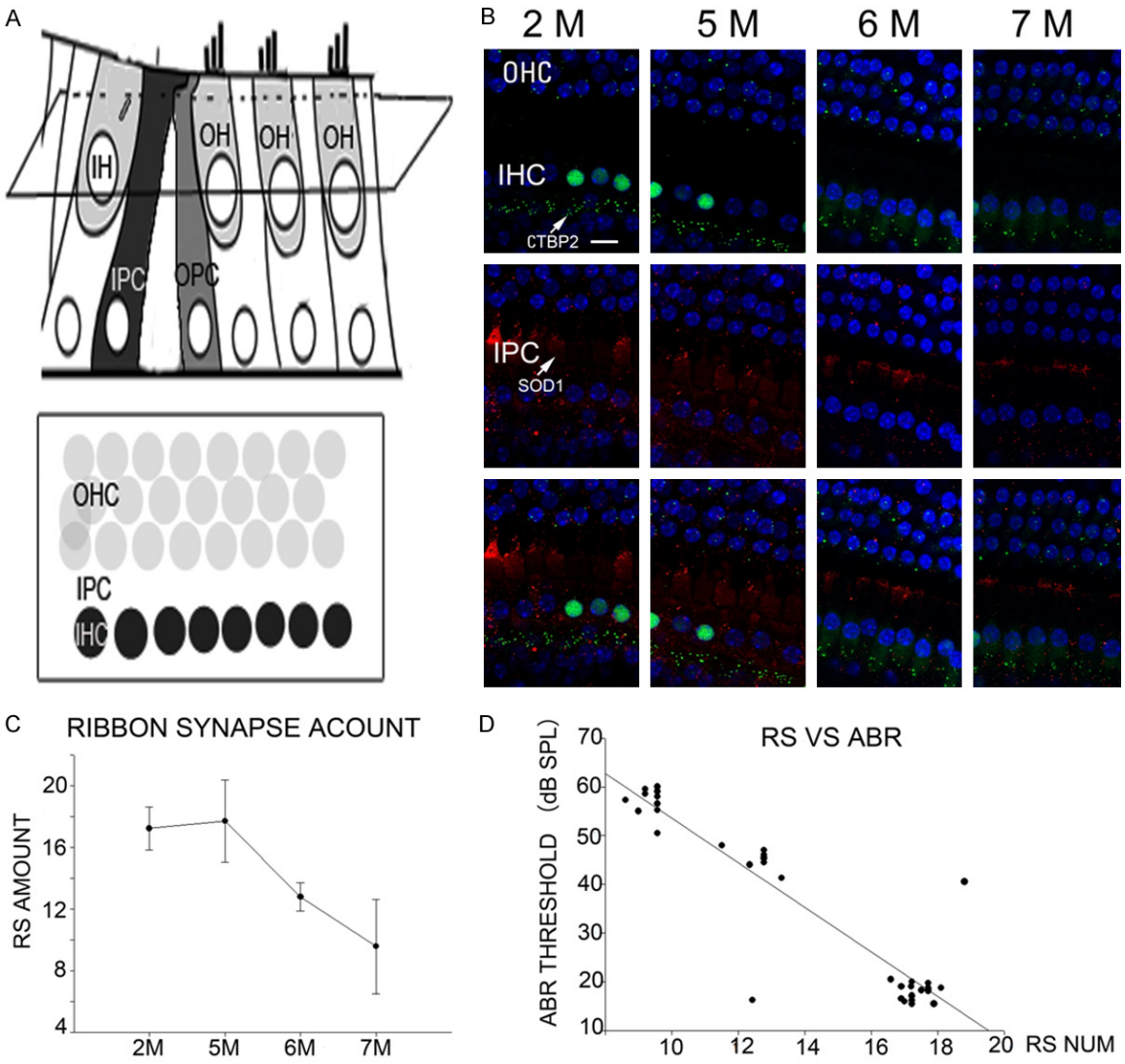

Figure 4. Changes in synaptic ribbons, SOD1 content in IPCs, and the relationships between the change of RS and the hearing threshold. A. The pattern diagram showed the structures of organ of Corti. A single row of IPCs was between the three-row OHCs and one-row IHCs. For the down location of IPCs nucleus, we could not see the IPCs nucleus in the sections. B. Pre-synaptic protein in the ribbon synapse (green spots) and SOD1 (red spots). The number of ribbon synapses decreased with age (bar = 25 μm). C. The mean number of ribbon synapses was 17.22 ± 1.4, 17.7 ± 2.67, 12.77 ± 0.92, and 9.56 ± 3.06 per IHC in the 2-, 5-, 6-, and 7-month groups, respectively. D. Linear regression analysis showed that changes in click auditory brainstem response (ABR) thresholds correlated with the number of ribbon synapses, with the maximal elevation of ABR thresholds being synchronized to the maximal loss of synapses.

Linear regression analysis revealed that changes in click-induced ABR thresholds correlated with the number of synapses and the peak ABR threshold coincided with the maximum loss of synapses (**Figure 4D**).

Discussion

The SOD1 antibody was used to detect the SOD1 protein. Of the three known isoforms of SOD, Cu/Zn SOD is the most abundant in the cochlea, comprising approximately 74% of the total SOD activity [9]. In Long-Evans rats, Cu/Zn SOD is distributed throughout the cochlea, with intense immunoreactivity in Reissner's membrane, the poststrial region of the spiral ligament, inner and outer hair cells, and the supporting cells of the organ of Corti [15].

SOD1 is the primary defense against free radical-induced damage. It converts the superoxide radical to less reactive hydrogen peroxide and

oxygen. Hydrogen peroxide is then further converted to water and oxygen by either catalase in the peroxisomes or GPX in the mitochondria and cytoplasm [16]. A failure to scavenge these oxidants leads to the damage of DNA, lipids, and proteins [17]. The damaged lipids can then lead to calcium influx and further cellular pathological changes [18, 19]. In our study, we found that the SOD1 content in the cochlea obviously declined with growth, demonstrating an age-related deficiency in oxidative scavenging function. In accordance with the Western blot data, frozen sections showed that SOD1 expression in the IHCs and IPCs reduced with age. McFadden *et al*. reported that unlike wild mice, SOD1-knockout mice had deteriorated hearing, implying that SOD1 deficiency led to the degeneration of cochlear hair cells, which proved that oxidative stress is early indicator of age-related changes of the cochlear [6].

Moreover, oxidative stress induces the hyperphosphorylation of tau proteins through the inactivation of protein phosphatase 1 and 2A, causing abnormal tau aggregation and blocking synaptic vesicle trafficking [20]. Thus, low SOD1 levels lead to the deficient scavenging of mitochondrial ROS, which in turn results in significant synaptic injury.

This is the first study to report on the changes in the expression of SOD1 in the IPCs of aging cochlea. The amount of SOD1 expressed in the IPCs is small and not easily observed. Our study implicated besides the traditional pathway as above, decreased SOD1 expression in IPC plays an important role in reducing sound transduction. The tunnel of Corti and PCs are unique mammalian structures. As supporting cells, one of the primary functions of IPCs is to nourish and support IHCs. The columnar epithelial cells that contain very large apico-basally-oriented transcellular microtubule bundles [10]. They provide excellent opportunities for analysis of the assembly of cell surface-associated microtubule arrays. Pillar cell microtubules are connected to sensory hair cells by substantial cell junctions at the pillar cell apices. The basal ends of pillar microtubules help to anchor hair cells to a basement membrane that does not make direct contact with the hair cells [21]. A tunnel formed by IPCs occurs in response to selective pressures related to increased auditory acuity and perception of high frequencies [22]. Hence, the micromechanical properties of pillar cells and their microtubules must inevitably have a marked influence on the acoustically-promoted vibrations of hair cells and electroneurographic signal transmissions [10], which is by the ribbon synapse. There is a high concentration of microtubule ends in the subapical layer, especially near its edges. To support the energy requirement, high metabolism should occur in the subapical edge of IPCs. This hypothesis was supported by our findings that highly concentrated SOD1 is observable in the apical portions of the IPCs.

The loss of the cochlear hair cells and SGNs is the foundation of permanent hearing loss, as these cells do not regenerate after death. Moreover, hair cell death is followed by the secondary loss of SGNs, as the afferent dendrites of the SGNs retract [23]. In older mice that have never been exposed to loud noises, the reduction in the afferent SGN-IHC innervation precedes SGN loss, suggesting that the ribbon synapse is the one of the primary sites of pathological changes in ARHL [24].

Whether the OHC or the ribbon synapse is the primary target of presbycusis remains unclear. A number of studies have found that ribbon synapses are vulnerable to noise and ototoxic chemicals [11, 13], but other studies have indicated that DPOAEs changed first in presbycusis [25, 26]. Interestingly, the first change that we detected in our study was in the DPOAE amplitudes at high frequencies, which occurred at the age of 5 months. Although a small decrease in low-frequency OHCs was detected in the 5-month group, the relevant DPOAE amplitudes did not change. We believe that this may be due to the four-line structure of the OHCs in the cochlear apex, which contributes to a higher compensatory ability. However, no shift in ABR thresholds was detected at this time. Elevation of the ABR thresholds was detected in 6-month-old mice and was accompanied by an obvious decrease in ribbon synapses. Linear regression analysis revealed that changes in click ABR thresholds were correlated with the total number of ribbon synapses. A significant decrease in hair cells occurred at nearly 7 months. Thus, impaired OHC function preceded ribbon synapse loss in ARHL.

In a recent study, Parthasarathy and Kujawa [27] found that a progressive decrease in coch-

lear synapses causing deficits in temporal coding was the main cause of ARHL in CBA/CaJ mice, and also contributed to supra-threshold sound processing. Furthermore, the authors found that the changes in synapses preceded those in the hair cells. This difference may have resulted from the use of different animal species. The C57BL/6J (C57) mouse strain is a model of early-onset hearing loss, while the CBA mouse strain is a model of relatively late-onset hearing loss. Compared with CBA mice, C57 mice showed earlier onset of high-frequency hearing loss and decreased OHC function, especially in high-frequency regions. One study compared DPOAE and morphological changes between CBA and C57 mice, and found that C57 mice exhibited more severe pathological changes within the cochlea and significantly lower OHC lengths in all three OHC rows in the basal turn than CBA mice of the same age [28].

It has been reported that in C57BL/6J mice, hearing disorders are first identified around 6-10 months of age [29], which is consistent with our results. We analyzed the SOD1 content in the organ of Corti and showed that SOD1 is primarily expressed in the IHCs and inner pillar cells. This expression was downregulated with increasing age and hearing loss. These findings are consistent with oxygen free radical theory and support the notion that ozone therapy, antioxidant treatment, fasting or other actions can inhibit cell damage or promote cell survival [30].

It is rather unlikely that a single mechanism accounts for SOD1 decrease-induced ribbon synapse loss, considering the cumulative and multifactorial nature of the damage. Further studies are needed to deepen our understanding of ARHL, for example, presbycusis animal experiments, proteomics analyses, and high-throughput genome sequencing. Advances in the methods for delivering drugs to the inner ear may facilitate the development of new and better presbycusis therapies.

Conclusion

SOD1 is present in the organ of Corti and is especially high in IPCs. SOD1 levels in the cochlea are related to the hearing threshold. Since IPCs support the IHCs and the conduction of vibration from the external lymphatic fluid, decreased SOD1 levels in the IPCs may play a key role in ARHL. Inner hair cells release the ribbon synapse depending on the vibration excitation, so impaired function of the IPCs may reduce the overall neural transmission. This study demonstrates the initial change of DPOAE in aging cochlea. Although the decrease in DPOAE amplitude precedes ribbon synapse loss, the number of ribbon synapses is correlated with ABR thresholds. Our study revealed that in C57BL/6J mice, ARHL was caused by multi-site degeneration in the cochlea. However, there are no known methods for measuring the IPC vibration, and the exact mechanism by which IPCs affect IHCs requires further investigation.

Acknowledgements

We extend our gratitude to Wei Sun at SUNY at Buffalo for providing technological assistance and revising the manuscript. This work was supported by grants from the National Natural Science Foundation of China (81503372), the Education Fund of Liaoning Province (LQ2017-015), and the China Scholarship Council (2017-08210289).

Disclosure of conflict of interest

None.

Address correspondence to: Lin Shi and Mei Lv, Department of Otorhinolaryngology, The First Affiliated Hospital, Dalian Medical University, Dalian 116013, China. E-mail: shilin516@sina.com (LS); lv_mei@163.com (ML)

References

[1] Tadros SF, D'Souza M, Zhu X and Frisina RD. Gene expression changes for antioxidants pathways in the mouse cochlea: relations to age-related hearing deficits. PLoS One 2014; 9: e90279.
[2] Gates GA and Mills JH. Presbycusis. Lancet 2005; 366: 1111-1120.
[3] Sergeyenko Y, Lall K, Liberman MC and Kujawa SG. Age-related cochlear synaptopathy: an early-onset contributor to auditory functional decline. J Neurosci 2013; 33: 13686-13694.
[4] Beckman KB and Ames BN. The free radical theory of aging matures. Physiol Rev 1998; 78: 547-581.
[5] Beckman KB and Ames BN. Mitochondrial aging: open questions. Ann N Y Acad Sci 1998; 854: 118-127.
[6] McFadden SL, Ding D, Burkard RF, Jiang H, Reaume AG, Flood DG and Salvi RJ. Cu/Zn

SOD deficiency potentiates hearing loss and cochlear pathology in aged 129,CD-1 mice. J Comp Neurol 1999; 413: 101-112.
[7] Fortunato G, Marciano E, Zarrilli F, Mazzaccara C, Intrieri M, Calcagno G, Vitale DF, La Manna P, Saulino C, Marcelli V and Sacchetti L. Paraoxonase and superoxide dismutase gene polymorphisms and noise-induced hearing loss. Clin Chem 2004; 50: 2012-2018.
[8] Ohlemiller KK, Wright JS and Heidbreder AF. Vulnerability to noise-induced hearing loss in 'middle-aged' and young adult mice: a dose-response approach in CBA, C57BL, and BALB inbred strains. Hear Res 2000; 149: 239-247.
[9] McFadden SL, Ding D, Reaume AG, Flood DG and Salvi RJ. Age-related cochlear hair cell loss is enhanced in mice lacking copper/zinc superoxide dismutase. Neurobiol Aging 1999; 20: 1-8.
[10] Tucker JB, Paton CC, Richardson GP, Mogensen MM and Russell IJ. A cell surface-associated centrosomal layer of microtubule-organizing material in the inner pillar cell of the mouse cochlea. J Cell Sci 1992; 102: 215-226.
[11] Shi L, Liu K, Wang H, Zhang Y, Hong Z, Wang M, Wang X, Jiang X and Yang S. Noise induced reversible changes of cochlear ribbon synapses contribute to temporary hearing loss in mice. Acta Otolaryngol 2015; 135: 1093-1102.
[12] Wang H, Zhao N, Yan K, Liu X, Zhang Y, Hong Z, Wang M, Yin Q, Wu F, Lei Y, Li X, Shi L and Liu K. Inner hair cell ribbon synapse plasticity might be molecular basis of temporary hearing threshold shifts in mice. Int J Clin Exp Pathol 2015; 8: 8680-8691.
[13] Liu K, Jiang X, Shi C, Shi L, Yang B, Shi L, Xu Y, Yang W and Yang S. Cochlear inner hair cell ribbon synapse is the primary target of ototoxic aminoglycoside stimuli. Mol Neurobiol 2013; 48: 647-654.
[14] Jiang XW, Li XR and Zhang YP. Changes of ribbon synapses number of cochlear hair cells in C57BL/6J mice with age (Delta). Int J Clin Exp Med 2015; 8: 19058-19064.
[15] Rarey KE and Yao X. Localization of Cu/Zn-SOD and Mn-SOD in the rat cochlea. Acta Otolaryngol 1996; 116: 833-835.
[16] Park C, Ji HM, Kim SJ, Kil SH, Lee JN, Kwak S, Choe SK and Park R. Fenofibrate exerts protective effects against gentamicin-induced toxicity in cochlear hair cells by activating antioxidant enzymes. Int J Mol Med 2017; 39: 960-968.
[17] Dalle-Donne I, Rossi R, Colombo R, Giustarini D and Milzani A. Biomarkers of oxidative damage in human disease. Clin Chem 2006; 52: 601-623.
[18] Joseph JA, Denisova N, Fisher D, Bickford P, Prior R and Cao G. Age-related neurodegeneration and oxidative stress: putative nutritional intervention. Neurol Clin 1998; 16: 747-755.
[19] Joseph JA, Denisova N, Fisher D, Shukitt-Hale B, Bickford P, Prior R and Cao G. Membrane and receptor modifications of oxidative stress vulnerability in aging. Nutritional considerations. Ann N Y Acad Sci 1998; 854: 268-276.
[20] Kamat PK, Kalani A, Rai S, Swarnkar S, Tota S, Nath C and Tyagi N. Mechanism of oxidative stress and synapse dysfunction in the pathogenesis of alzheimer's disease: understanding the therapeutics strategies. Mol Neurobiol 2016; 53: 648-661.
[21] Gulley RL and Reese TS. Intercellular junctions in the reticular lamina of the organ of Corti. J Neurocytol 1976; 5: 479-507.
[22] Holley M. High frequency force generation in outer hair cells from the mammalian ear. Bioessays 1991; 13: 115-120.
[23] Wong AB, Jing Z, Rutherford MA, Frank T, Strenzke N and Moser T. Concurrent maturation of inner hair cell synaptic Ca2+ influx and auditory nerve spontaneous activity around hearing onset in mice. J Neurosci 2013; 33: 10661-10666.
[24] Sergeyenko TV and Los DA. Identification of secreted proteins of the cyanobacterium Synechocystis sp. strain PCC 6803. FEMS Microbiol Lett 2000; 193: 213-216.
[25] Zhu X, Vasilyeva ON, Kim S, Jacobson M, Romney J, Waterman MS, Tuttle D and Frisina RD. Auditory efferent feedback system deficits precede age-related hearing loss: contralateral suppression of otoacoustic emissions in mice. J Comp Neurol 2007; 503: 593-604.
[26] Park SN, Back SA, Park KH, Kim DK, Park SY, Oh JH, Park YS and Yeo SW. Comparison of cochlear morphology and apoptosis in mouse models of presbycusis. Clin Exp Otorhinolaryngol 2010; 3: 126-135.
[27] Parthasarathy A and Kujawa SG. Synaptopathy in the aging cochlea: characterizing early-neural deficits in auditory temporal envelope processing. J Neurosci 2018; 38: 7108-7119.
[28] Park SN, Back SA, Choung YH, Kim HL, Akil O, Lustig LR, Park KH and Yeo SW. alpha-Synuclein deficiency and efferent nerve degeneration in the mouse cochlea: a possible cause of early-onset presbycusis. Neurosci Res 2011; 71: 303-310.
[29] Chen L, Xiong S, Liu Y and Shang X. Effect of different gentamicin dose on the plasticity of the ribbon synapses in cochlear inner hair cells of C57BL/6J mice. Mol Neurobiol 2012; 46: 487-494.
[30] Wong AC and Ryan AF. Mechanisms of sensorineural cell damage, death and survival in the cochlea. Front Aging Neurosci 2015; 7: 58.